

*Article*

Experimental and Analytical Study on Reinforcing Steels with Threaded Mechanical Couplers under Monotonic and Cyclic Loadings

Pochara Kruavit^{1,a}, Anat Ruangrassamee^{2,b,*}, and Qudeer Hussain^{2,c}

¹ Department of Civil Engineering, Faculty of Engineering, Chulalongkorn University, Bangkok, 10330, Thailand

² Center of Excellence on Earthquake Engineering and Vibration, Department of Civil Engineering, Faculty of Engineering, Chulalongkorn University, Bangkok, 10330, Thailand

E-mail: ^aPochara.Kr@student.chula.ac.th, ^banat.r@chula.ac.th (Corresponding author),

^cebbadat@hotmail.com

Abstract. This study performs the experimental and analytical investigation on the effect of mechanical couplers on the axial behavior of spliced reinforcing bars. The effect of unsupported-length-to-bar-diameter (L/D) ratios on the monotonic and cyclic behavior was observed. The test configurations in monotonic tension, compression, and cyclic tests included reinforcing bars with and without threaded mechanical couplers. Specimens with mechanical couplers have higher strength in compression than the bars without couplers, especially when L/D is less than 10. The procedure for determining the effective unsupported length for bars with a mechanical splice was proposed. And the observation on the energy dissipation confirmed the proposed method. The calculated hysteretic loops using the modified unsupported length model of the bar with mechanical splice agreed well with the test result.

Keywords: Buckling, mechanical coupler, cyclic loading, reinforcing steel, OpenSees.

ENGINEERING JOURNAL Volume 24 Issue 3

Received 30 October 2019

Accepted 18 March 2020

Published 31 May 2020

Online at <https://engj.org/>

DOI:10.4186/ej.2020.24.3.61

1. Introduction

Reinforced concrete structures with seismic design typically allows plastic deformations of the structural elements, thus causing nonlinear behavior of steel reinforcement. The AASHTO Bridge Design Specifications [1] and Caltrans Seismic Design Criteria [2], prohibit all mechanical splices from being placed in plastic hinge regions. However, building design codes ACI 318-02 [3] allow Type 2 mechanical splices, which can develop the full tensile strength of the spliced bars to be placed at locations subjected to high inelastic demands.

One of mechanical splices, which is commonly referred to as “a coupler,” offer significant savings in terms of cost and a considerable reduction in the construction time comparison to lap splice. Couplers can be categorized as the mechanism of force transfer through the coupler system. Threaded couplers consist of male and female threaded steel collars, which transfer the force of compression and tension being transmitted directly through deformed heads and threaded collars, respectively.

Although couplers are extensively utilized in structural members, the application for couplers requires sufficient test data to be able to incorporate analytical modeling methods for mechanically spliced RC components. The performance of RC member incorporating mechanical bar splices were tested by using up-set headed coupler [4], grouted sleeve couplers [5], shear screw couplers [6-7], headed bar couplers [8], swaged couplers [9] and threaded coupler [10]. The effect of mechanical splices on the behaviors of structural members were investigated to ensure the performance of structural members in terms of strength and ductility under seismic loading. [11-15]. However, the stress-strain relation of reinforcing bars with couplers under compression and cyclic loading is very limited and deserves further detailed investigation.

This study focuses on the behavior of the reinforcing steels with threaded mechanical couplers under monotonic and cyclic loadings. The effect of 1) bar diameter, 2) unsupported-length-to-bar-diameter ratios (L/D) are investigated in detail. Then the analytical model is proposed for the application in structural analysis.

2. Experimental Investigation

2.1. Specimen Details

The threaded mechanical splice system used in this study consists of male threaded reinforcing bars and female threaded steel coupler that joins bar segments as shown in Fig. 1. The force in the bars is transferred through the deformed heads for compression and the threaded coupler for tension. To assemble the threaded mechanical splicing system, an initial torque of approximately 200 N-m is needed, as specified by the manufacturer. The mechanical splice system used in the study is classified as Type 2 according to ACI 318.

The reinforcing bar with and without threaded mechanical splices were investigated in this study. The

tested deformed bars have diameters of 20, 25, and 32 mm and Grade SD40 manufactured according to TIS24-2015 [16]. The average of three tests was used to obtain a typical tensile stress-strain relation for each bar size. The L/D ratios for the compression test were 10, 12, and 16 while the L/D ratios for cyclic loading were 10 and 16 as shown in Table 1.

The material properties of bars are summarized in Table 2. The average tensile yield strength (f_y) of deformed bar with diameters of 20, 25, and 32 mm are 407, 498, and 473 MPa respectively. The ultimate tensile strength (f_u) are 625, 639, and 622 MPa, respectively.

2.2. Test Setup and Loading Scheme

All specimens were tested using the Instron 1000kN servo-hydraulic controlled universal testing machine. The monotonic compression loading was carried out under displacement-control, according to ASTM A1034 [17]. Cyclic loading was conducted using the loading scheme as shown in Fig. 2. The test setup simulated the longitudinal reinforcing bar with restraint at the supports, as shown in Fig. 3. The unsupported length was measured as the distance between load frame grips of universal testing machine. The strain was measured directly using digital extensometer mounted with 200 mm gauge length at the middle portion of the specimen. The average strain measured by three displacement transducers were used to determine axial displacements.

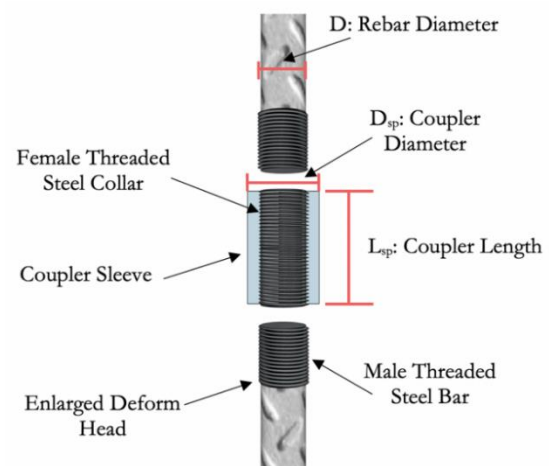


Fig. 1. Parallel-threaded mechanical splice system.

Table 1. Parameters for the experiment

Specimens ID	DB			MS		
Rebar size (mm)	20	25	32	20	25	32
Coupler Diameter (mm)	-	-	-	32	41	50
Coupler Length (mm)	-	-	-	54	70	80
L/d	Compression			10, 12, 16		
	Cyclic			- 10, 16		

*deformed bars are denoted in the following as DB20, DB25 and DB32, while spliced bars are denoted in the following as MS20, MS25, and MS32, respectively.

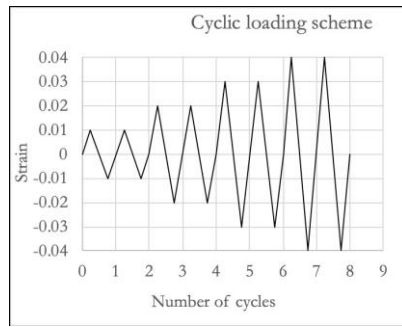


Fig. 2. Cyclic test loading scheme.

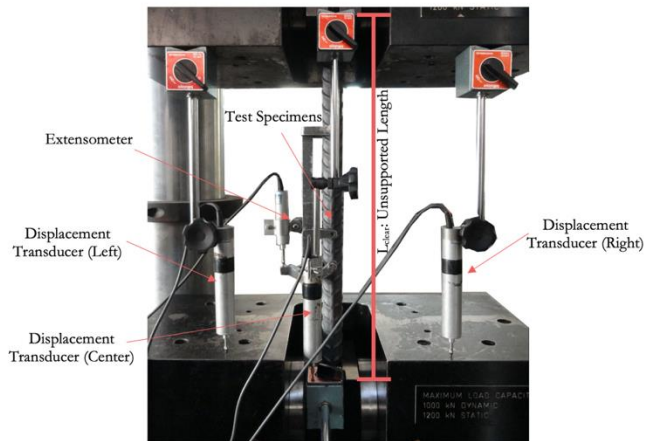


Fig. 3. Uniaxial test setup.

3. Test results and Discussions

Experimental results obtained from tensile and compression tests are summarized in Table 2. For tension tests, experimental data is summarized in terms of yield strength, ultimate strength, modulus of elasticity, yielding strain in linear and nonlinear regions. Whereas, for compression tests, experimental data is summarized in terms of ultimate strength and strain corresponding to the ultimate strength. The experimental results indicate that tensile behavior of both deformed bar specimens and spliced specimens is almost identical in terms of yield strength and ultimate strength. Tensile strengths of both deformed bar and spliced specimens are almost the same. This is because both deformed bar and spliced specimens mainly failed due to the tensile rupture of the steel bars. Further, it is observed in compression tests that the compressive stress of spiced specimens is higher than the deformed bar specimens. The specimens with mechanical splice in compression test have the improvement in post-yield softening branch in compression, which strongly influences the cyclic behavior of the bar. For the larger L/D ratio, load-carrying capacity dropped rapidly with increasing strains. Some studies [18-20] reported that the inelastic buckling behavior of a reinforcing bar was very sensitive to the unsupported L/D ratio. Experimental results in terms of stress versus strain relations are discussed in detail in the following sections.

3.1. Monotonic Tensile Test

The yield strength and ultimate strength obtained from control bars and coupler specimens were almost identical in all diameter because rupture occurred within in the reinforcing bars as shown in Fig. 4. No damage to the coupler sleeve was observed but loss of tightness was found at the connection after the bar rupture. The stress-strain relationship of deform bars shows yielding and ultimate strengths close to those of deform bars. As seen from Fig.5, the modulus of elasticity of the spliced specimen is less than that of the control bar because the deformation of the thread and coupler itself.

Table 2. Tensile and compressive properties of deform bar and spliced specimens.

ID	Tension				
	Elastic region		Inelastic region		
	Yield strength (MPa)	ϵ_y	E (GPa)	ϵ_{sh}	Ultimate strength f_u (MPa)
DB20	407	0.0020	203	0.0120	625
DB25	498	0.0025	197	0.0075	639
DB32	473	0.0024	193	0.0124	622
MS20	408	0.0032	127	0.0096	653
MS25	501	0.0045	109	0.0075	642
MS32	479	0.0054	87	0.0124	632

ID	Compression					
	Unsupported length to bar diameter (L/D) ratio					
	10		12		16	
	Ult. Stress (MPa)	Strain at Ult. Stress	Ult. Stress (MPa)	Strain at Ult. Stress	Ult. Stress (MPa)	Strain at Ult. Stress
DB20	405	0.0048	413	0.0049	402	0.0031
DB25	517	0.0051	474	0.0044	490	0.0039
DB32	472	0.0073	473	0.0043	450	0.0036
MS20	488	0.0115	405	0.0048	403	0.0068
MS25	585	0.0201	479	0.0073	467	0.0036
MS32	553	0.0147	474	0.0058	472	0.0041

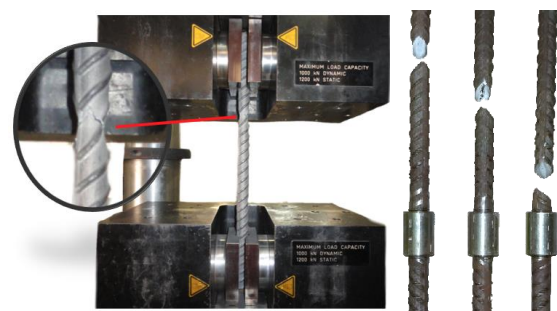


Fig. 4. Tension failure of specimen.

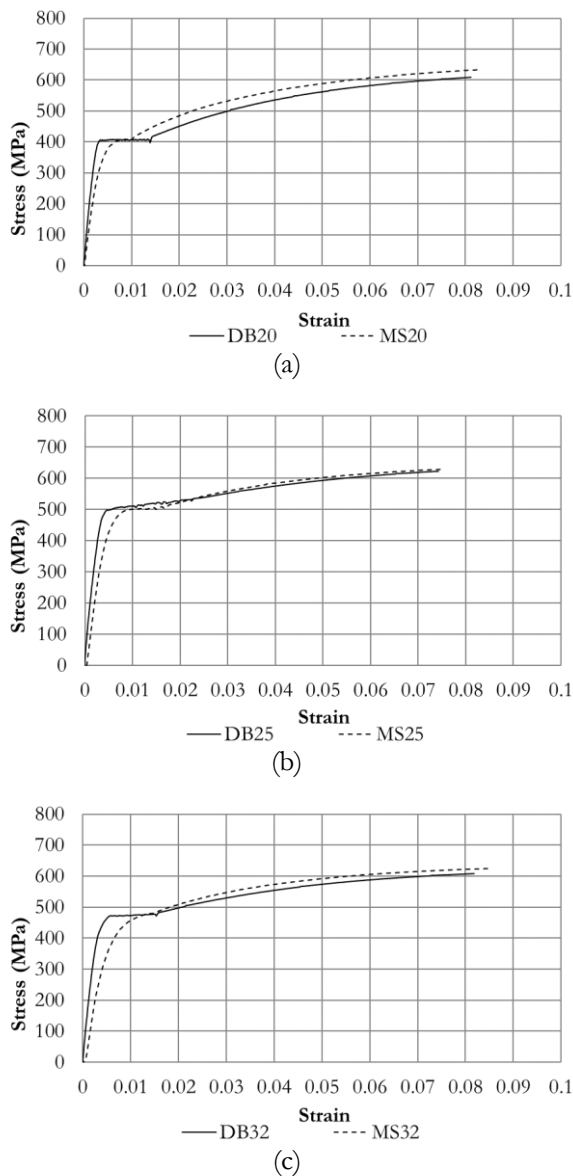


Fig. 5. Stress-strain relationship (Tension) of deform bar and coupler specimens (a) DB20 vs MS20, (b) DB25 vs MS25, (c) DB32 vs MS32.

3.2. Monotonic Compressive Test

The monotonic compressive test of deformed bar and spliced specimens with different diameters of 20, 25, and 32 mm and L/D ratios of 10, 12, and 16 were conducted. The difference in post-yield softening branch after buckling result was observed as shown in Fig. 6. The specimens with larger L/D ratios had a sudden drop of load-carrying capacity after the buckling. The shape of specimens at the end of the test is shown in Fig. 7. The significant buckling obviously occurs outside the coupler where the stiffness is significantly higher. The compressive strength for the L/D ratio equal to 10 was larger than the yield strength of the bars. The compressive strength for the L/D ratio equal to 16 was close to the yield strength and buckling occurred prematurely.

The normalized stress-strain relation shown in Fig. 8 illustrates the slope of post buckling behavior for different

L/D ratios. Clearly, the coupler can improve the behavior of reinforcing bar under compression by having higher capacity after yielding.

The energy absorption in terms of strain energy was investigated for different L/D ratios, as shown in Fig. 9 and summarized in Table 3. It is seen that the energy dissipation is significantly improved. The spliced bar with L/D=12 has the energy dissipation close to that of the deformed bar with L/D=10.

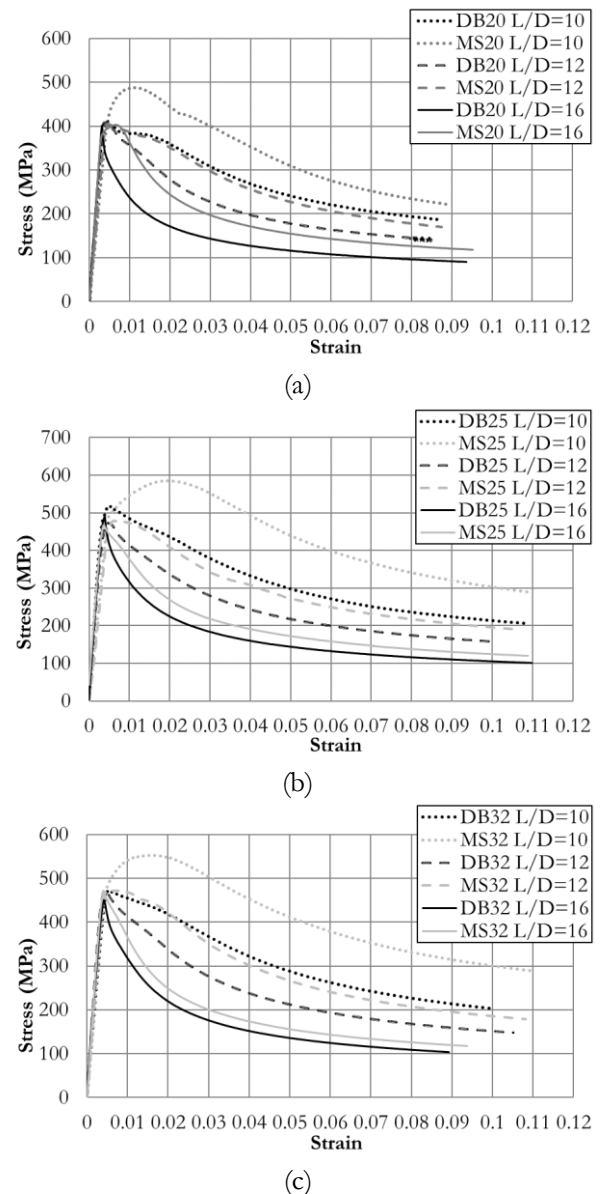


Fig. 6. Stress-strain relationship of deform bar and spliced specimens under compression (a) DB20 vs MS20, (b) DB25 vs MS25, (c) DB32 vs MS32.

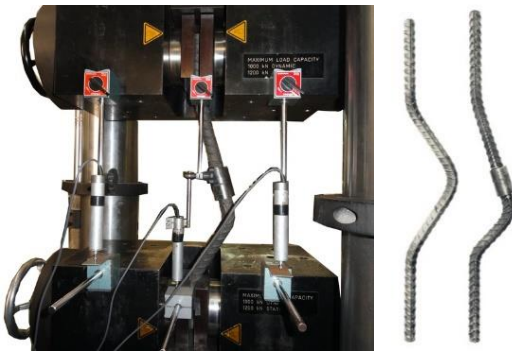


Fig. 7. Buckling shape of specimens under monotonic compression test.

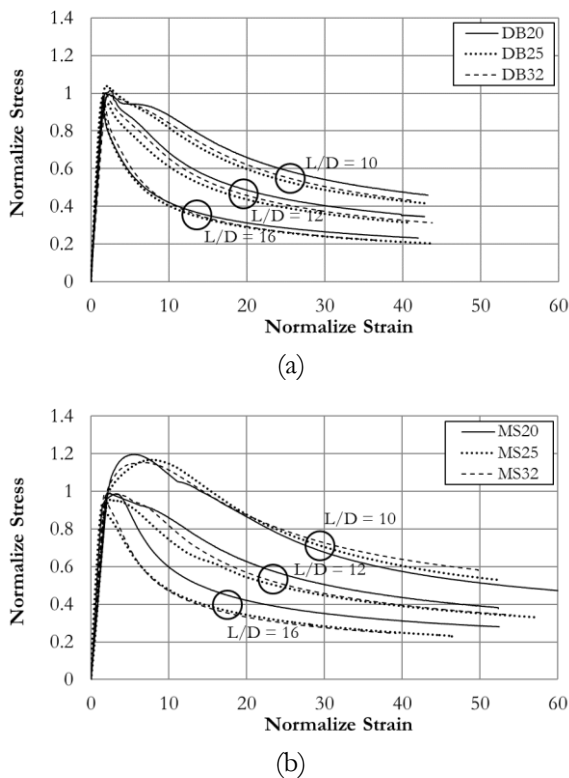


Fig. 8. Normalized stress - strain for (a) deformed bar and (b) spliced specimens.

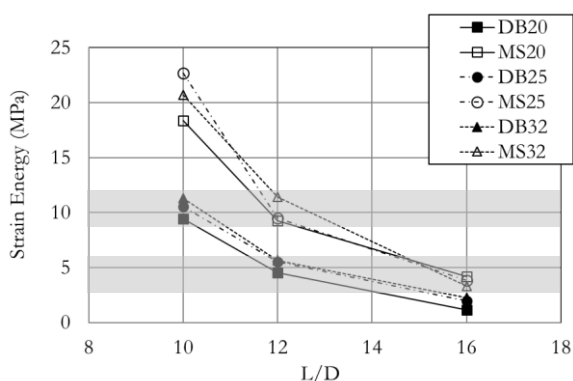


Fig. 9. Relationship of strain energy and L/D ratios of deform bars and spliced specimens.

Table 3. Summary of strain energy.

ID	Strain Energy (MPa)			
	L/D	10	12	16
DB20		9.41	4.54	1.16
MS20		18.35	9.24	4.18
DB25		10.52	5.54	1.94
MS25		22.69	9.47	3.83
DB32		11.30	5.65	2.28
MS32		20.68	11.45	3.29

3.3. Cyclic Loading Test

The cyclic loading test was conducted using the loading scheme in Fig. 2. After the test, some specimens failed in low-cycle fatigue fracture as shown in Fig. 10. The hysteretic loops for all specimens are shown in Fig. 11. The lower strength in compression is due to the buckling of reinforcing bars. The transition between tension to compression occurred with explicit pinching behavior. The hysteretic loop is smaller for bars with a larger L/D ratio.



Fig. 10. Fracture failure of MS25 (L/D = 10, 16).

4. Proposed Unsupported Length of Spliced Reinforcing Bars

As observed from failure of spliced specimens throughout the test, buckling and failure occurred outside the couplers since the couplers were much stiffer in flexure than the bar. Hence, it is proposed that the unsupported length of reinforcing bar with mechanical splices is determined by the clear unsupported length (L_{clear}) subtracted by the length of the mechanical splice (L_{sp}), which is considered rigid against buckling, as shown in Fig. 12. Table 4 shows L/D ratios based on the proposed unsupported length. Referring to the cyclic loading test result in Fig. 9, the L/D ratio based on the proposed unsupported length yields the result close to the test. For example, the L/D ratio of 10 for the deformed bar gives the result in terms of strain energy close to the spliced bar with the L/D ratio of 12. And the proposed

unsupported length $(L_{\text{clear}} - L_{\text{sp}})/D$ for the specimen is about 9.5 which is close to 10.

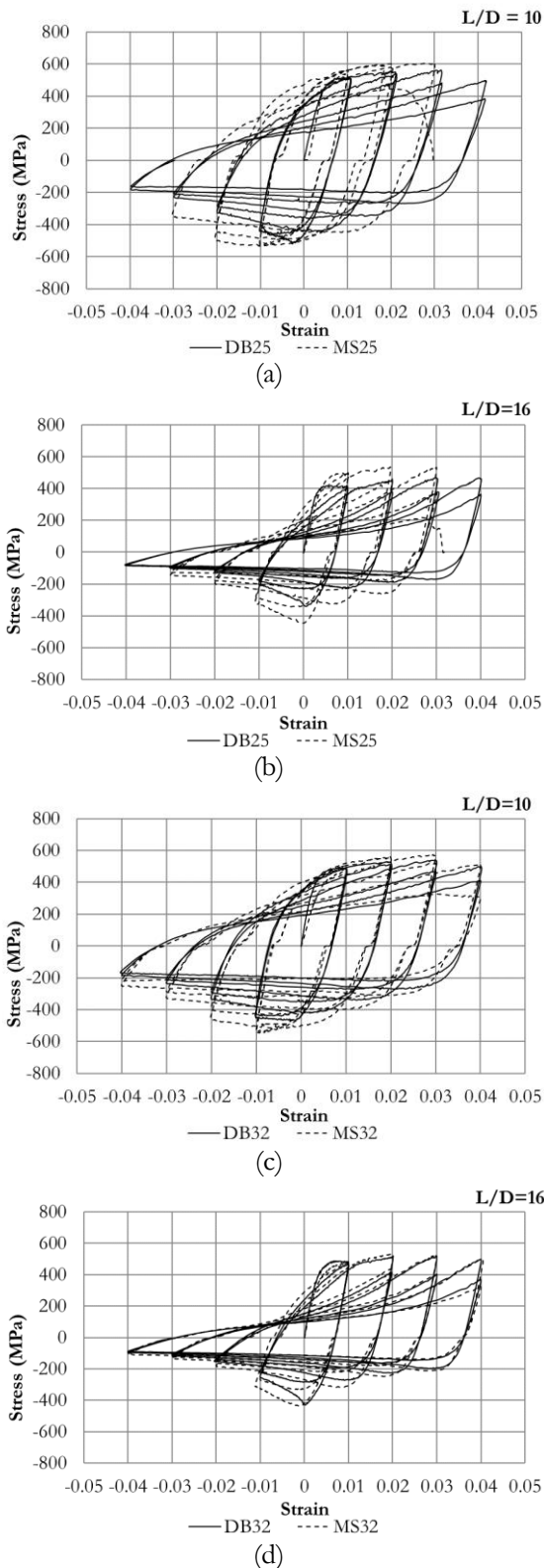


Fig. 11. Stress-strain relationship for different bar diameters and L/D ratios under cyclic loading.

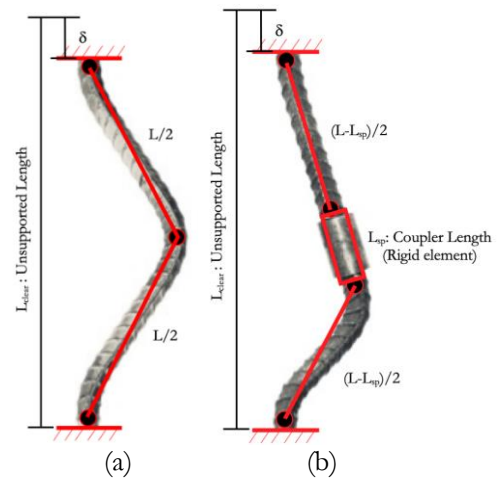


Fig. 12. Buckling mechanism of (a) deformed bar and (b) spliced reinforcing bar.

Table 4. L/D ratios based on proposed unsupported length

	L_{clear}/D		
DB20,25,32	10	12	16
	$(L_{\text{clear}}-L_{\text{sp}})/D$		
MS20	7.3	9.3	13.3
MS25	7.2	9.2	13.2
MS32	7.5	9.5	13.5

A numerical model was developed using the OpenSees program [21]. The reinforcing bars material properties were defined using the uniaxial material model called “ReinforcingSteel”. The Gomes–Appleton (1997) model which is the average stress–strain relationship including buckling was used [22]. In the material model, the buckling behavior is represented by some parameters: β is a factor to scale the buckling curve; γ factor is the positive stress location about which the buckling factor is initiated; r factor is used to adjust the buckled curve. In the study the values used are $\beta=1$, $\gamma=0$ and $r=0.15$. The reinforcing bar was model as the beam element with fiber sections that the ReinforcingSteel uniaxial material was assigned, as shown in Fig. 13. The axial load was applied by using displacement control with a strain increment of 0.001.

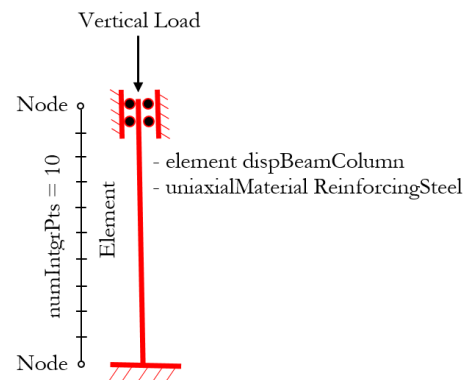


Fig. 13. Numerical models of reinforcing bar with and without mechanical splice.

5. Experimental Verification

The proposed model was validated using test results discussed previously for threaded mechanical splices. The constitutive model was calibrated using average measured material properties as in Table. 2. To demonstrate the effectiveness of the numerical model, the test results of specimens in cyclic tests are compared with the theoretical predictions using the Gomes–Appleton model and the proposed unsupported length of mechanical splice, respectively, as shown in Figs. 14 and 15.

Eight reinforcing steels with and without mechanical splice under reversed cyclic loading were used for verification. A good correlation is observed between unloading and reloading paths of the calculated hysteresis and the measured curve. The solid lines represent the experimental results, whereas dashed lines represent the numerical results

The energy dissipation is compared in Table. 5. The calculated energy dissipation of mechanical splice is generally higher than the reinforcing bar. This is mainly because the predicted compression load is higher in the model result. The parameters which predicts buckling behaviors deserves further investigation.

6. Conclusions

Reinforcing steels with threaded mechanical couplers were evaluated under monotonic tension, monotonic compression and cyclic loading tests. Various sizes of bars, L/D ratios were investigated. The stress-strain relations were obtained from the test. Then the model was proposed based on observed response. Based on the results, the following conclusions can be made:

- 1) In this study, various diameters of specimen bars were employed. The displacement ductility response was observed, and test results clearly showed that the coupler sleeve can improve the buckling behavior of reinforcing bar under compression force. The test results were stable and consistent with the variables studied.
- 2) The procedure proposed for determining the effective unsupported length for bars with a mechanical splice was proposed. And the observation on the energy dissipation confirmed the proposed method.
- 3) The calculated hysteretic loops using the modified unsupported length model of the bar with mechanical splice agreed reasonably with the test result.

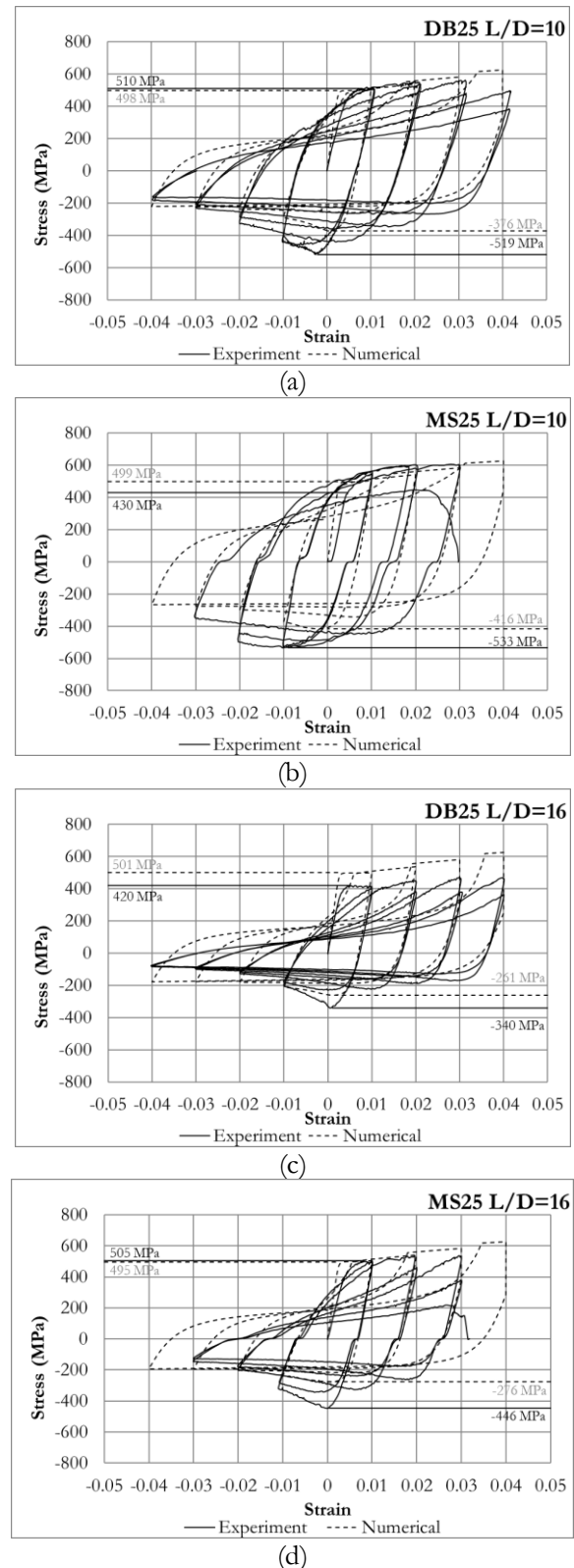


Fig. 14. Comparison of numerical predictions and experimental results (a) Specimen DB25 L/D=10, (b) Specimen MB25 L/D=10, (c) Specimen DB25 L/D=16 a

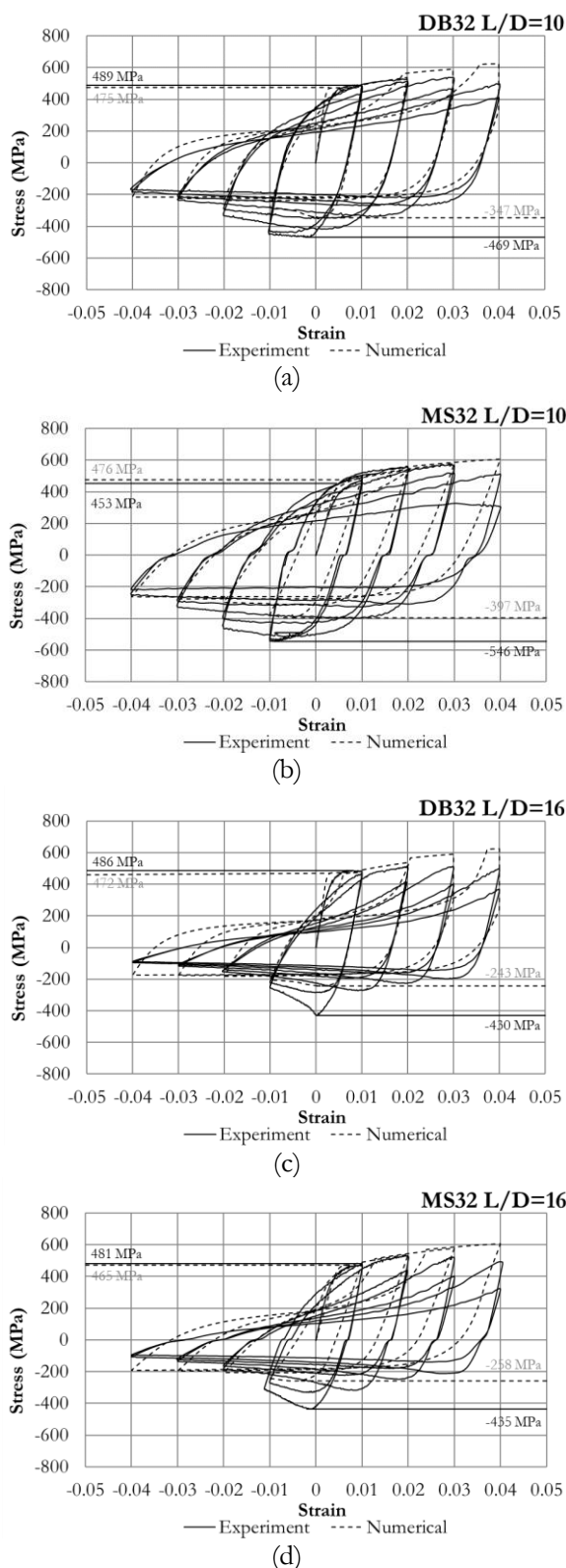


Fig. 15. Stress-strain relationship (Cyclic) of (a) DB25 vs MS25 with $L/d = 10$ and (b) $L/d = 16$, (c) DB32 vs MS32 with $L/d = 10$ and (d) $L/d = 16$.

Table 5. Strain energy of Experimental and Numerical model.

	L/D	Strain Energy (MPa) at a certain strain					
		Experiment			Numerical model		
		0.01	0.02	0.03	0.01	0.02	0.03
DB25	10	21.43	66.86	128.00	9.53	29.16	56.65
MS25	10	17.23	70.49	150.00	10.45	33.39	66.18
DB25	16	14.03	36.86	66.15	7.92	24.23	46.58
MS25	16	17.80	35.36	84.63	8.27	26.00	50.64
DB32	10	19.75	63.63	120.15	9.09	27.73	55.12
MS32	10	16.08	63.04	127.03	6.00	23.81	52.31
DB32	16	16.52	42.89	77.55	7.57	23.24	45.34
MS32	16	17.50	47.15	82.99	4.93	19.21	41.12

Acknowledgement

This research is supported by the Thailand Research Fund (TRF). The authors would like to thank Dextra Manufacturing Co. Ltd. for providing materials for the tests.

References

- [1] American Association of State Highway and Transportation Officials (AASHTO), "AASHTO Guide Specifications for LRFD Seismic Bridge Design", 2nd edition, Washington, DC, 2011.
- [2] State of California Department of Transportation, "Caltrans Seismic Design Criteria Version 2.0," CA, 2019.
- [3] American Concrete Institute, "Building Code Requirements for Structural Concrete and Commentary (ACI 318-19)," MI, 2019.
- [4] Z. B. Haber, M. S. Saïdi, and D. H. Sanders, "Seismic performance of precast columns with mechanically spliced column-footing connections," *ACI Structural Journal*, vol. 111, no. 3, pp. 639-650, 2014.
- [5] A. A. Hashib, "Effects of Mechanical Bar Splices on Seismic Performance of Reinforced Concrete Buildings," M.S. Thesis, South Dakota State University, SD, 2017.
- [6] W. R. Lloyd, "Qualification of the bar-lock rebar coupler for use in nuclear safety-related applications mechanical testing program and performance analysis," Report No. INEEL/EXT-02-01387, Idaho National Engineering and Environmental Laboratory, ID, 2001.
- [7] D. Hillis and M. S. Saïdi, "Construction and nonlinear dynamic analysis of three bridge bents used in a bridge system test," Report No. CCEER-09-03, University of Nevada, Reno, NV, 2009.
- [8] Z. B. Haber, M. S. Saïdi and D. H. Sanders, "Behavior and simplified modeling of mechanical

- reinforcing bar splices,” *ACI Structural Journal*, vol. 112, no. 2, pp. 179, 2015.
- [9] Y. Yang, L. H. Sneed, M. S. Saiidi, and A. Belarbi, “Repair of earthquake-damaged bridge columns with interlocking spirals and fractured bars,” Caltrans, CA, 2014.
- [10] D. E. Lehman, S. E. Gookin, A. M. Nacamuli, and J. P. Moehle, “Repair of earthquake-damaged bridge columns,” *ACI Structural Journal*, vol. 98, no. 2, pp. 233-242, 2001.
- [11] C. A. Cruz-Noguez and M. S. Saiidi, “Performance of advanced materials during earthquake loading tests of a bridge system,” *Journal of Structural Engineering*, vol. 139, no. 1, pp. 144-154, 2013.
- [12] M. J. Ameli, J. E. Parks, D. N. Brown, and C. P. Pantelides, “Seismic evaluation of grouted splice sleeve connections for reinforced precast concrete column-to-cap beam joints in accelerated bridge construction,” *PCI Journal*, vol. 60, no. 2, pp. 80-103, 2015.
- [13] Z. B. Haber, M. S. Saiidi, and D. H. Sanders, “Behavior and simplified modeling of mechanical reinforcing bar splices,” *ACI Structural Journal*, vol. 112, no. S16, pp. 179-188, 2015.
- [14] O. Vasile and O. Tonciu, “Static and dynamic tests for determining the characteristic performance of mechanical splices in reinforced concrete,” 35th *Danubia Adria Symposium on Advances in Experimental Mechanics*, Romania, pp. 97-98, 2018.
- [15] M. Tazarv and M. S. Saiidi, “Seismic design of bridge columns incorporating mechanical bar splices in plastic hinge regions,” *Engineering Structures*, vol. 124, pp. 507-520, 2016.
- [16] Thai Industrial Standards Institute, “TIS24 Steel bars for reinforced concrete: deformed bars,” 2016.
- [17] ASTM International, “ASTM A1034/A1034M Standard Test Methods for Testing Mechanical Splices for Steel Reinforcing Bars,” PA, 2015.
- [18] G. Monti and C. Nuti, “Nonlinear cyclic behavior of reinforcing bars including buckling,” *Journal of Structural Engineering*, vol. 118, no. 12, pp. 3268-3284, 1992.
- [19] S. Bae, A. M. Miseses, and O. Bayrak, “Inelastic buckling of reinforcing bars,” *Journal of Structural Engineering*, vol. 131, no. 2, pp. 314-321, 2005.
- [20] E. Cosenza and A. Prota, “Experimental behaviour and numerical modelling of smooth steel bars under compression,” *Journal of Earthquake Engineering*, vol. 10, no. 3, pp. 313-329, 2006.
- [21] S. Mazzoni, F. McKenna, M. H. Scott, and G. L. Fenves, “OpenSees command language manual,” Pacific Earthquake Engineering Research Center, University of California, Berkeley, CA, 2009.
- [22] A. Gomes and J. Appleton, “Nonlinear cyclic stress-strain relationship of reinforcing bars including buckling,” *Engineering Structures*, vol. 19, no. 10, pp. 822-826, 1997.



Pochara Kruavit was born in Thailand in 1987. He received the B.Eng. degree in Civil Engineering from Chiangmai University, Thailand, in 2010 and the M.Eng. degree in Civil Engineering from Chulalongkorn University, Thailand, in 2013.

Since 2013, he was a Research Assistant at the Center of Excellence on Earthquake Engineering and Vibration, Civil Engineering Department, Faculty of Engineering, Chulalongkorn University, Thailand.

His research interests include seismic behaviour of reinforced concrete members, strengthening of reinforced concrete structures and nonlinear analysis of reinforced concrete structures.



Anat Ruangrassamee was born in Bangkok, Thailand in 1976. He received the B.Eng. degree in Civil Engineering from Chulalongkorn University in 1996, the M.Eng. degree in Civil Engineering from Tokyo Institute of Technology in 1998, and the Ph.D. degree in Civil Engineering from Tokyo Institute of Technology in 2001.

Since 2001, he has worked at Department of Civil Engineering, Chulalongkorn University and is currently an Associate Professor. His research interests include seismic design of bridges, tsunami modelling, effect of tsunamis on structures.



Qudeer Hussain was born in Pakistan in 1979. He received the B.S. and M.S. degrees in Civil Engineering from the University of Engineering and Technology Taxila, Pakistan in 2009 and the Ph.D. degree in Civil Engineering/Structural Engineering from Thammasat University, Thailand, in 2015.

From 2015 to 2016, he was a Research Associate with Sirindhorn International Institute of Technology, Thammasat University, Thailand. From 2016 to 2017, he was a Lecturer at Kasem Bunding University, Thailand. From 2017 to 2019, he was a Research Faculty Member at Construction and Maintenance Technology Research Center (CONTEC), School of Civil Engineering and Technology, Sirindhorn International Institute of Technology, Thammasat

University, Thailand. Since September 2019, he has been a Post-Doctoral Researcher with Civil Engineering Department, Faculty of Engineering, Chulalongkorn University, Thailand. His research interests include structural dynamics and earthquake engineering, nonlinear behavior and modeling of reinforced concrete structures and seismic retrofitting of reinforced concrete buildings.